Protective role of protease-activated receptor-2 in anaphylaxis model mice

Short title: Protease-activated receptor-2 in anaphylaxis

Maho Nakazawa[1], Ryota Tochinai[2], Wataru Fujii[3], Tomohiro Yonezawa[1], Yasuyuki Momoi[1], Shingo Maeda[1 *]

[1] Department of Veterinary Clinical Pathobiology, Graduate School of Agricultural and Life Sciences, The University of Tokyo, Tokyo, Japan

[2] Department of Veterinary Pathophysiology and Animal Health, Graduate School of Agricultural and Life Sciences, The University of Tokyo, Tokyo, Japan

[3] Laboratory of Biomedical Science, Graduate School of Agricultural and Life Sciences, The University of Tokyo, Tokyo, Japan

[*] Corresponding author

E-mail: amaeda@g.ecc.u-tokyo.ac.jp（S M）

Abstract

Anaphylaxis is a severe life-threatening hypersensitivity reaction induced by mast cell degranulation. Among the various mediators of mast cells, little is known about the role of tryptase. Therefore, we aimed to elucidate the role of protease-activating receptor-2 (PAR-2), a receptor activated by tryptase, in murine anaphylactic models using PAR-2-deficient mice and newly generated tryptase-deficient mice. Anaphylaxis was induced by IgE-dependent and IgE-independent mast cell degranulation in mice. PAR-2 deficiency exacerbated the decrease in body temperature and hypotension during anaphylaxis; however, the number of skin mast cells, degree of mast cell degranulation, and systemic and local vascular hyperpermeability were comparable in PAR-2 knockout and wild-type mice. Nitric oxide, which is produced by endothelial nitric oxide synthase (eNOS), is an indispensable vasodilator in anaphylaxis. In the lungs of anaphylactic mice, PAR-2 deficiency promoted eNOS expression and phosphorylation, suggesting a protective effect of PAR-2 against anaphylaxis by downregulating eNOS activation and expression. Based on the hypothesis that the ligand for PAR-2 in anaphylaxis is mast cell tryptase, tryptase-deficient mice were generated using CRISPR-Cas9. In wild-type mice, the PAR-2 antagonist exacerbated the body temperature drop due to anaphylaxis; however, the effect of the PAR-2 antagonist was abolished in tryptase-deficient mice. These results suggest that tryptase is a possible ligand of PAR-2 in anaphylaxis and that the tryptase/PAR-2 pathway attenuates the anaphylactic response in mice.

Introduction

Anaphylaxis is a severe, life-threatening systemic hypersensitivity reaction characterized by rapid onset of airway, breathing, or circulatory problems [1]. Food, insect venom, and drugs constitute the most common elicitors of anaphylaxis worldwide [1]. Although the mechanism is not fully understood, mast cells and their mediators play a crucial role in the onset of anaphylaxis. Mast cells can be activated by elicitors in an immunoglobulin E (IgE)-dependent or IgE-independent manner and release mediators such as histamine, platelet-activating factor (PAF), prostaglandin D2 (PGD2), and proteases such as tryptase and chymase. These mediators act orchestrally on endothelial and smooth muscle cells, resulting in severe vascular hyperpermeability and vasodilation [2]. Histamine has been reported to increase vascular permeability mainly by nitric oxide (NO)-dependent vasodilation and subsequent increases in blood flow and endothelial barrier dysfunction [3,4]. In addition, PAF can contribute to both vascular hyperpermeability and vasodilation by activating endothelial nitric oxide synthase (eNOS) and promoting NO production [5]. However, antihistamines have limited effects in patients with anaphylaxis [6], and PAF receptor antagonism cannot completely inhibit hypotension in a rat anaphylaxis model [7], suggesting that the function of known mediators alone does not fully explain the pathogenesis of anaphylaxis and that other mediators are involved.

Tryptase is the most abundant protein in human mast cells [8]. Since tryptase is released by mast cell degranulation, serum tryptase concentration has been reported to correlate with the severity

of anaphylaxis and is a useful biomarker for the diagnosis of anaphylaxis [9–11]. However, little is known about the role of tryptase in anaphylaxis pathogenesis. In this study, we focused on protease-activated receptor-2 (PAR-2), a tryptase-activated receptor. PAR-2 is a member of the protease-activated receptor family and is activated by specific serine proteases such as mast cell tryptase, trypsin, factor Xa (FXa), and FVIIa, which cleave the N-terminus of the receptor [12]. PAR-2 is widely expressed in intestinal and airway epithelial cells, endothelial cells, and smooth muscle cells [13]. Activation of PAR-2 in endothelial cells has been reported to modulate VE-cadherin expression and affect vascular barrier function *in vitro* [14]. In addition, PAR-2 appears to be involved in both endothelium-dependent relaxation and contraction [15]. In this study, we investigated the effects of PAR-2 on anaphylactic symptoms in murine models of anaphylaxis.

Materials and Methods

Ethics statement

All animal experiments were approved by the Animal Care and Use Ethical Committees of the Graduate School of Agricultural and Life Sciences, University of Tokyo (approval no. P19-135 and P20-122H02).

75 # Regents

76 Compound 48/80, Evans blue dye, anti-DNP-specific IgE, and DNP-albmin were purchased from
77 Sigma Aldrich (St. Louis, MO, USA). Selective PAR-2 antagonist (ENMD-1068) was purchased from
78 MedChemExpress (Monmouth Junction, NJ, USA).

79

80 # Mice

81 Wild-type (WT) C57BL6/J and ICR mice were purchased from Sankyo Labo Service Corporation
82 (Tokyo, Japan). PAR-2 KO mice were purchased from Jackson Laboratories (Bar Harbor, ME, USA).
83 The tryptases released by mast cells in mice are mouse mast cell protease-6 (mMCP-6) and mouse
84 mast cell protease-7 (mMCP-7) [8]. In humans, δ-tryptase, the ortholog of mMCP-7, is mostly inactive
85 [16]. Wild-type C57BL/6 mice are genetically deficient in *mMCP-7* [17], thus, mMCP-6 deficiency
86 in C57BL/6 mice also implies systemic tryptase deficiency. *mMCP-6* knockout C57BL/6J mice
87 (mMCP-6 KO) were generated by CRISPR/Cas9-mediated genome editing in zygotes, according to
88 previous reports [18,19].

89

90 # Passive systemic anaphylaxis model

91 Anti-DNP-specific-IgE (clone: SPE-7, 10 μg/head) was intravenously injected into WT and PAR-2
92 KO mice, followed 18 h later by intravenous injection with DNP-albumin (300 μg/head). The rectal

93 temperature was measured every 5 min for 60 min using a thermometer (Physitemp, NJ, USA).

94

95 IgE-independent anaphylaxis model

96 C48/80 (2 mg/kg) in 100 μL saline was administered intravenously to the WT, PAR-2 KO, and
97 mMCP-6 KO mice. In some experiments, ENMD-1068 (10 mg/kg) or saline was injected
98 intraperitoneally 30 min before the C48/80 injection. Rectal temperature was measured every 5 min
99 for 60 min.

100

101 Mast cell staining and immunofluorescence staining for 102 mMCP-6 in skin

103 The mouse ears were fixed in 10% formamide and embedded in paraffin. Sections (2 μm) were
104 deparaffinized and autoclaved at 121 °C for 10 min in 10 mM sodium citrate buffer (pH 6.0). The
105 sections were blocked with 5% skimmed milk in TBS-T at room temperature for 60 min and then
106 incubated with rabbit anti-mMCP-6 antibody (R&D Systems, MN, USA, 1:500) at 4 °C overnight.
107 After washing with TBS, sections were incubated with secondary antibody (Alexa Fluor 594 goat anti-
108 rat IgG, Abcam, 1:500) and FITC-avidin (BioLegend, CA, USA, 1:200) for 1 h at room temperature
109 and counterstained with DAPI. FITC-avidin was used to label mast cells in the skin. Images were
110 captured using a BZ-X800 fluorescence microscope (KEYENCE, Osaka, Japan). The digitized images

111 were transferred to a computer to measure the size of each region using a software (ImageJ, National
112 Institute of Mental Health, MD, USA), and FITC-positive mast cells were counted. The results are
113 expressed as positive cells per mm^2.
114

115 Hematocrit, histamine, and mMCP-6 measurement

116 Blood samples were obtained 10 min after intravenous administration of C48/80 (2 mg/kg) to measure
117 the hematocrit, plasma histamine, and mMCP-6 levels. To determine hematocrit levels, blood was
118 collected in heparinized microhematocrit tubes (DRUMMOND, PA, USA) and centrifuged at 12,000
119 rpm for 3 min. The ratio of red blood cell volume to total blood volume was determined using a
120 hematocrit reader. Plasma histamine and mMCP-6 levels were measured using a histamine EIA kit
121 (Bertin Bioreagent, Montigny-le-Bretonneux, France) and Mcpt6 ELISA kit (Thermo Fisher Scientific,
122 MA, USA), respectively.
123

124 Vascular permeability assay

125 To evaluate systemic vascular permeability, blood was collected from WT and PAR-2 KO mice 10
126 min after vehicle or C48/80 (2 mg/kg) injection. In other experiments, C48/80 (2 mg/kg) with 0.5%
127 Evans blue dye was intravenously administered to WT or PAR-2 KO mice, while the control mice
128 received Evans blue only. Thirty minutes after injection, the lungs were collected and weighed. The

129 extravasated Evans blue was extracted in formamide at 56 °C for 24 h. The concentration of Evans
130 blue was quantified spectrophotometrically at 620 nm using a plate reader (iMark microplate reader,
131 Bio-Rad, CA, USA). To assess local vascular permeability in the skin, C48/80 (100 ng in 20 μL saline,
132 right ear) or saline (left ear) was intradermally injected into the mouse ear. Evans blue (0.5% in 100
133 μL saline) was injected intravenously 5 min after intradermal anaphylactic stimulation. After 30 min,
134 the ear was dissected and Evans blue leakage was measured as described above.
135

136 Blood pressure measurement

137 The mice were anesthetized with 1.5% isoflurane and placed in the supine position on a plate heated
138 to 37 °C. The left femoral artery was exposed and a polyethylene catheter filled with heparinized saline
139 was inserted. The catheter was connected to a transducer amplifier (Nihon Kohden, Tokyo, Japan)
140 through a pressure transducer (NEC Sanei, Tokyo, Japan), and the arterial pressure was recorded.
141 Mean blood pressure was continuously sampled at intervals of 1 ms using an analysis system (SBP-
142 2000, Softron, Tokyo, Japan) with an analog-to-digital converter connected in series to a personal
143 computer. During the blood pressure recording period, a single dose of C48/80 (2 mg/kg) was
144 administered through the right femoral vein. Blood pressure was recorded for up to 30 min after
145 administration.
146

147 # Expression of eNOS mRNA

148 The lungs of mice were excised before and 1 h after the injection of C48/80 (2 mg/kg). Total RNA
149 was extracted from tissues using NucleoSpin RNA (Takara Bio, Shiga, Japan) according to the
150 manufacturer's instructions. Reverse transcription was performed using a commercially available kit
151 (ReverTra Ace with gDNA remover; TOYOBO, Osaka, Japan). Real-time PCR of eNOS and β-actin
152 was performed using a commercially available kit (THUNDERBIRD Next SYBR qPCR Mix;
153 TOYOBO). The following primer sets were used: eNOS, forward 5'-
154 CAACGCTACCACGAGGACATT-3' and reverse 5'-CTCCTGCAAAGAAAAGCTCTGG-3'; β-
155 actin, forward 5'-GGAAATCGTGCGTGACATCA-3' and reverse 5'-
156 GCCACAGGATTCCATACCCA-3'. The PCR reaction consisted of 40 cycles, each for 30 s at 95 °C,
157 followed by 5 s at 95 °C, and 10 s at 60 °C. The expression level of eNOS was normalized to that of
158 β-actin as a reference gene, and the values were calculated relative to the baseline of the WT mice,
159 which was converted to 1.

160

161 # Western blot

162 C48/80 (2 mg/kg) was administered intravenously to WT and PAR-2 KO mice, and the lungs were
163 collected before administration and at 10 and 120 min after administration. The lungs were
164 homogenized in RIPA buffer (50 mmol/L Tris-HCl [pH 7.4], 150 mmol/L NaCl, 5 mmol/L EDTA,

165 1% Triton X-100, 10 mmol/L NaF) containing protease and phosphatase inhibitor cocktails (Wako,
166 Osaka, Japan). For the detection of eNOS and phosphorylated eNOS, the samples (25 μg per lane)
167 were separated by electrophoresis and transferred to PVDF membranes.
168 The membranes were blocked with 5% BSA at room temperature for 30 min and incubated with anti-
169 eNOS (clone: D9A5L, Cell Signaling Technology, MA, USA, 1:1,000) and anti-Ser177 p-eNOS
170 (clone: C9C3, Cell Signaling Technology, 1:1,000) antibodies. Samples were also probed with an anti-
171 β-actin antibody (GeneTex, CA, USA, 1:1,000) to normalize protein loading. The membrane was then
172 incubated with secondary antibody (donkey anti-rabbit IgG IRDye 680, LICOR Biosciences, NE, USA,
173 1:10,000) at room temperature for 1 h. The bands were quantified using the Odyssey Imaging System
174 (LICOR Biosciences).
175

176 Statistical analysis

177 Data are expressed as mean±SEM, and all experiments were repeated at least three times. Statistical
178 analyses were performed using R software (version 4.2.1). Two-way repeated ANOVA was used to
179 compare the degree of temperature reduction between the two groups. For blood pressure comparisons,
180 a two-way repeated ANOVA was performed at two time points: before C48/80 administration and at
181 the time of blood pressure measurement. Skin mast cell counts, serum histamine and mMCP-6
182 concentrations, and lung eNOS and phosphorylated eNOS expression were analyzed using Student's *t*

183 test. Vascular permeability and lung eNOS gene expression in anaphylaxis model mice were analyzed

184 using Tukey's test. Statistical significance was defined as $P < 0.05$.

185

186

187

188 Results

189 PAR-2 deficiency exacerbates IgE-dependent and IgE-

190 independent anaphylaxis in mice without affecting vascular

191 permeability

192 To verify the effect of PAR-2 on the decrease in body temperature during IgE-dependent anaphylaxis,

193 passive systemic anaphylaxis was induced in the WT and PAR-2 KO mice. IgE-mediated anaphylaxis

194 was more severe in PAR-2 KO mice than in WT mice, as determined by the decrease in body

195 temperature (Fig 1A). Consistent with this finding, intravenous injection of C48/80 induced a more

196 severe decrease in body temperature in PAR-2 KO mice than in WT mice (Fig. 1B). These data

197 indicate that PAR-2 deficiency exacerbates the decrease in body temperature during IgE-dependent

198 and IgE-independent anaphylaxis.

199 Next, we examined the number of mast cells in WT and PAR-2 KO mice. There was no

200 significant difference in the number of mast cells in the skin between WT and PAR-2 KO mice (S1

201 Fig). To further investigate whether the level of mast cell degranulation differed between WT and
202 PAR-2 KO mice, plasma histamine and mast cell tryptase (mMCP-6) levels were measured after
203 injection of C48/80. There was no significant difference in plasma histamine and mMCP-6 levels
204 between WT and PAR-2 KO mice (S1 Fig).

205 During anaphylaxis, mast cell mediators such as histamine and PAF induce vascular
206 hyperpermeability, leading to hypotension and hypothermia. We investigated the extent of systemic
207 and local vascular hyperpermeability induced by C48/80 in WT and PAR-2 KO mice. First, the
208 hematocrit was measured in WT and PAR-2 KO mice treated with vehicle or C48/80. In both WT and
209 PAR-2 KO mice, C48/80 injection significantly increased the hematocrit level compared to vehicle
210 injection. However, there was no significant difference in hematocrit between WT and PAR-2 KO
211 mice after vehicle or C48/80 injection (S2 Fig). In addition, PAR-2 deficiency did not affect Evans
212 blue dye leakage in the lungs after systemic C48/80 injection (S2 Fig). Next, we examined the effect
213 of PAR-2 on local vascular permeability after the local injection of C48/80 into the auricles of mice.
214 The results showed that Evans blue leakage was significantly increased in C48/80-treated auricles
215 compared to that in solvent-treated auricles, in both WT and PAR-2 KO mice. However, there was no
216 significant difference in the amount of pigment leakage in the auricles of WT and PAR-2 KO mice
217 (S2 Fig). These results suggest that PAR-2 has little effect on systemic and local vascular
218 hyperpermeability induced by C48/80.

219

220 **Fig 1. PAR-2 deficiency exacerbates the body temperature during IgE-dependent and IgE-**

221 **independent anaphylaxis.** (A) Decrease in body temperature during IgE-dependent anaphylaxis in

222 WT and PAR-2 KO mice (n = 5 each). (B) Decrease in body temperature during IgE-independent

223 anaphylaxis in WT and PAR-2 KO mice (n = 4 each). *P <0.05. ***P < 0.001. Data are presented as

224 mean ± SEM.

225

226 PAR-2 deficiency exacerbates hypotension in mice with 227 anaphylaxis

228 Hypotension is the hallmark of anaphylaxis. We investigated whether PAR-2 deficiency could affect

229 hypotension induced by C48/80 injection. In WT mice under anesthesia, the mean arterial blood

230 pressure decreased rapidly within 10 min after C48/80 injection and then recovered. PAR-2 KO mice

231 also showed a rapid decrease in blood pressure, but the recovery was slower than that in WT mice and

232 began to recover 30 min after C48/80 injection. Blood pressure in PAR-2 KO mice was significantly

233 lower than that in WT mice 15 and 20 min after C48/80 injection (Fig 2).

234

235 **Fig 2. PAR-2 deficiency exacerbates blood pressure in IgE-independent anaphylaxis.** Arterial

236 blood pressure after injection of C48/80 in WT and PAR-2 KO mice (n = 8-9). *P < 0.05. Data are

237 presented as the mean ± SEM.

238

239 PAR-2 deficiency increases eNOS expression and 240 phosphorylation during anaphylaxis *in vivo*

241 The decrease in body temperature and hypotension in anaphylaxis are caused by a synergistic effect
242 of increased vascular permeability and decreased vascular resistance due to vasodilation. Previous
243 studies have suggested that PAR-2 deficiency does not affect vascular permeability during anaphylaxis.
244 Therefore, we hypothesized that PAR-2 deficiency may be involved in vasodilation during
245 anaphylaxis. eNOS and its product, NO, have been reported to be important for the decrease in body
246 temperature and hypotension in the anaphylaxis model.

247 First, gene expression levels in WT and PAR-2 KO mice were evaluated. In WT mice, there was no
248 significant difference in eNOS gene expression in the lungs before and after C48/80 administration.
249 However, in PAR-2 KO mice, eNOS gene expression in the lungs after C48/80 injection was
250 significantly higher than that before C48/80 injection (Fig 3A). Next, eNOS expression and
251 phosphorylation in the lung were quantified by western blotting. At baseline, there was no significant
252 difference in the protein expression and phosphorylation levels of eNOS between WT and PAR-2 KO
253 mice (Fig 3B). In contrast, 120 min after C48/80 injection, the expression level of eNOS was
254 significantly higher in PAR-2 KO mice than in WT mice (Fig 3C). Furthermore, 10 min after C48/80

255 injection, PAR-2 KO mice showed a significantly higher level of eNOS phosphorylation in the lungs
256 than WT mice (Fig 3C). These results suggest that PAR-2 deficiency causes activation of eNOS
257 through phosphorylation and a subsequent increase in eNOS protein expression during anaphylaxis.
258
259 **Fig 3. PAR-2 deficiency promotes eNOS expression and phosphorylation in IgE-independent**
260 **anaphylaxis.** (A) Relative gene expression of eNOS in the lungs of WT and PAR-2 KO mice before
261 (0 min) and 60 min after (60 min) C48/80 injection (n = 4 each). (B) Expression and phosphorylation
262 levels of eNOS in lungs of WT and PAR-2 KO mice at baseline (n = 4–5). (C) Expression and
263 phosphorylation levels of eNOS in lungs of WT and PAR-2 KO mice after injection of C48/80 (n =
264 4–5). NS, not significant. *$P < 0.05$. Data are presented as mean ± SEM.
265

266 Mast cell protease-6 is a possible ligand for PAR-2 in 267 anaphylaxis

268 We hypothesized that mast cell tryptase, mMCP-6, is the ligand that activates PAR-2 during
269 anaphylaxis. Therefore, we generated mMCP-6 KO mice using the CRISPR/Cas9 system. Two
270 gRNAs were used to delete exon2 of mMCP-6, which contains the start codon and is essential for
271 mMCP-6 expression (Fig 4A). The designed gRNAs and Cas9 mRNA were then microinjected into
272 C57BL/6J-derived zygotes. The zygotes were then transferred into the oviductal ampulla of 0.5 dpc

273 pseudopregnant ICR females. After obtaining pups by natural birth, the genotypes were confirmed by
274 genome PCR-directed sequencing (Fig 4A). A pup with exon2 deleted and a small indel was
275 backcrossed several times with wild-type C57BL/6J mice, and the offspring were subjected to the
276 following experiments. The phenotype of mMCP-6 KO mice was confirmed by immunofluorescence
277 of the skin. In WT mice, mMCP-6 protein was detected in mast cells (avidin-FITC-positive cells, Fig
278 4B). In mMCP-6 KO mice, although there was a comparable level of mast cells in the skin as in WT
279 mice, no mMCP-6 expression was observed (Fig 4B).

280 To evaluate the effect of mMCP-6 on anaphylaxis, WT and mMCP-6 KO mice were
281 intravenously injected with C48/80. Contrary to our expectation, there was no significant difference
282 in body temperature decrease between WT and mMCP-6 KO mice (Fig 4C). To test whether mMCP-6
283 is involved in the suppression of anaphylaxis through PAR-2 activation, we compared the effects of a
284 PAR-2 antagonist (ENMD-1068) on C48/80-induced anaphylaxis in WT and mMCP-6 KO mice.
285 Administration of the PAR-2 antagonist exacerbated the decrease in body temperature during
286 anaphylaxis in WT mice (Fig 4D), whereas administration of the PAR-2 antagonist did not affect the
287 decrease in body temperature (Fig 4E).

288

289 **Fig 4. mMCP-6 deficiency abolishes the effect of the PAR-2 antagonist on anaphaylaxis.** (A) Map
290 of mMCP-6 gene and targeting region exon 2. (B) Immunofluorescence of mMCP-6 and mast cell

291 staining in ear skin of WT and mMCP-6 KO mice (magnification, ×400). Bar, 50 μm. (C) IgE-
292 independent anaphylaxis in WT and mMCP-6 KO mice (n = 5 each). (D) The effect of pre-treatment
293 with PAR-2 antagonist in WT mice with IgE-independent anaphylaxis (n = 4 each). (E) The effect of
294 pre-treatment with PAR-2 antagonist in mMCP-6 KO mice with IgE-independent anaphylaxis (n = 4
295 each). NS, not significant. *$P < 0.05$. Data are presented as the mean ± SEM.
296
297

298 # Discussion

299 The present study on anaphylaxis mouse models provides evidence supporting that PAR-2 has a
300 protective effect on acute decreases in body temperature and hypotension. PAR-2 deficiency did not
301 affect the number of mast cells in the skin or the concentrations of serum histamine and mMCP-6,
302 suggesting that PAR-2 may be involved in the acute response after mast cell degranulation rather than
303 in mast cell degranulation itself. In addition, the results showed that PAR-2 signaling negatively
304 controlled the phosphorylation and production of eNOS during anaphylaxis, possibly resulting in the
305 maintenance of body temperature and blood pressure during anaphylaxis. It is highly possible that the
306 ligand of PAR-2 during anaphylaxis is mast cell tryptase, mMCP-6; however, further research is
307 needed to confirm this finding. These results provide novel evidence of the role of PAR-2 in protecting
308 the body from life-threatening anaphylaxis.

309 C48/80 is known to activate mast cells independent of IgE via the Mas-related G protein-
310 coupled receptor b2 (Mrgprb2; mouse ortholog of human MrgprX2) [20]. The two types of mast cell
311 degranulation, IgE-dependent and IgE-independent, differ in their kinetics and duration of mediator
312 release [21,22]. In the present study, PAR-2 deficiency exacerbated the decrease in body temperature
313 in both IgE-dependent and IgE-independent anaphylaxis, suggesting that PAR-2 is involved in
314 downstream of both IgE-dependent and independent degranulation.

315 In anaphylaxis, vascular hyperpermeability is an important factor in the exacerbation of
316 symptoms, and several reports using anaphylaxis mouse models have shown a relationship between
317 vascular hyperpermeability and decreased body temperature [23,24]. Although PAR-2 deficiency
318 exacerbated the symptoms of anaphylaxis, the systemic and local vascular permeability in PAR-2 KO
319 mice was comparable to that in WT mice. These results are consistent with those of asthma and atopic
320 dermatitis models using PAR-2 antagonist and PAR-2 KO mice [25,26]. Since PAR-2 is thought to
321 have less effect on vascular permeability in anaphylaxis, we focused on vasodilation, which is also
322 crucial for the decrease in body temperature and hypotension. NO production following eNOS
323 phosphorylation is one of the most important factors for vasodilation [5,24,27]. Phosphorylation of
324 eNOS at Ser1177 has been reported to be important for eNOS activation during anaphylaxis in mice
325 [5,28]. This study showed that PAR-2 deficiency increased the phosphorylation and expression of
326 eNOS *in vivo* after the injection of C48/80. PAR-2 has been reported to be expressed in endothelial

327 cells [13]. Therefore, endothelial PAR-2 may suppress eNOS phosphorylation during anaphylaxis.
328 Although some reports have shown that PAR-2 activation results in the phosphorylation of eNOS at
329 Ser1177 in human endothelial cells and rat aorta with metabolic syndrome [29–31], another study
330 reported that PAR-2 suppressed eNOS phosphorylation at Ser1177 in the aorta of diabetic mice [32].
331 Taken together with the results of our study, the effect of PAR-2 on the phosphorylation and activation
332 of eNOS differs depending on the condition of the body. The downstream pathway by which PAR-2
333 inhibits eNOS phosphorylation remains unclear. It has been reported that phosphatase and tensin
334 homolog deleted on chromosome 10 (PTEN), a PIP_3 phosphatase, negatively controls eNOS
335 phosphorylation via Akt, and a rapid decrease in PTEN activity is known to cause an increase in eNOS
336 activation in a murine anaphylaxis model [33]. A previous report showed that PAR-2 activation
337 induces PTEN release and regulates PTEN activity in some cell lines [34]. Further studies are required
338 to clarify the mechanisms by which PAR-2 inhibits eNOS activation during anaphylaxis.

339 Based on our hypothesis that mast cell tryptase was the ligand for PAR-2 during anaphylaxis,
340 tryptase-deficient (mMCP-6 KO) mice were generated. Contrary to our expectations, mMCP-6
341 deficiency had no effect on body temperature drop in C48/80-induced anaphylaxis. However, the
342 effect of the PAR-2 antagonist, which exacerbated the decrease in body temperature in the anaphylaxis
343 model, was abolished in mMCP-6 KO mice, suggesting that mMCP-6 may be involved in the
344 inhibitory effect of PAR-2 on anaphylactic symptoms. In addition, these results indicate that the role

of mMCP-6 in anaphylaxis is not restricted to that of PAR-2. In humans, tryptase has been reported to have the potential to exacerbate the anaphylaxis by promoting the bradykinin production [35–37].

In conclusion, we showed for the first time that PAR-2 has inhibitory effects on the decrease in body temperature and blood pressure during anaphylaxis, possibly via the upregulation of eNOS phosphorylation and expression. Therefore, PAR-2 agonism may be a potential therapeutic target for anaphylaxis.

Acknowledgements

This study was supported by JSPS KAKENHI, a Grant-in-Aid for Science Research (Grant Number:19H00968), and Anicom Capital Research Grant (EVOLVE). We would like to thank Editage (www.editage.com) for English language editing.

355 # References

356 1. Cardona V, Ansotegui IJ, Ebisawa M, El-Gamal Y, Fernandez Rivas M, Fineman S, et al.
357 World allergy organization anaphylaxis guidance 2020. World Allergy Organ J. 2020;13:
358 100472. doi:10.1016/j.waojou.2020.100472

359 2. Nguyen SMT, Rupprecht CP, Haque A, Pattanaik D, Yusin J, Krishnaswamy G. Mechanisms
360 Governing Anaphylaxis: Inflammatory Cells, Mediators, Endothelial Gap Junctions and
361 Beyond. Int J Mol Sci. 2021;22. doi:10.3390/IJMS22157785

362 3. Ashina K, Tsubosaka Y, Nakamura T, Omori K, Kobayashi K, Hori M, et al. Histamine
363 Induces Vascular Hyperpermeability by Increasing Blood Flow and Endothelial Barrier
364 Disruption In Vivo. PLoS One. 2015;10. doi:10.1371/JOURNAL.PONE.0132367

365 4. di Lorenzo A, Fernández-Hernando C, Cirino G, Sessa WC. Akt1 is critical for acute
366 inflammation and histamine-mediated vascular leakage. Proc Natl Acad Sci U S A. 2009;106:
367 14552–14557. doi:10.1073/PNAS.0904073106

368 5. Cauwels A, Janssen B, Buys E, Sips P, Brouckaert P. Anaphylactic shock depends on PI3K
369 and eNOS-derived NO. J Clin Invest. 2006;116: 2244–2251. doi:10.1172/JCI25426

370 6. Gabrielli S, Clarke A, Morris J, Eisman H, Gravel J, Enarson P, et al. Evaluation of Prehospital
371 Management in a Canadian Emergency Department Anaphylaxis Cohort. J Allergy Clin
372 Immunol Pract. 2019;7: 2232-2238.e3. doi:10.1016/J.JAIP.2019.04.018

373 7. Tacquard C, Oulehri W, Collange O, Garvey LH, Nicoll S, Tuzin N, et al. Treatment with a
374 platelet-activating factor receptor antagonist improves hemodynamics and reduces epinephrine
375 requirements, in a lethal rodent model of anaphylactic shock. Clin Exp Allergy. 2020;50: 383–
376 390. doi:10.1111/CEA.13540
377 8. Caughey GH. Mast cell tryptases and chymases in inflammation and host defense. Immunol
378 Rev. 2007;217: 141–154. doi:10.1111/j.1600-065X.2007.00509.x
379 9. de Schryver S, Halbrich M, Clarke A, la Vieille S, Eisman H, Alizadehfar R, et al. Tryptase
380 levels in children presenting with anaphylaxis: Temporal trends and associated factors. J
381 Allergy Clin Immunol. 2016;137: 1138–1142. doi:10.1016/J.JACI.2015.09.001
382 10. Sala-Cunill A, Cardona V, Labrador-Horrillo M, Luengo O, Esteso O, Garriga T, et al.
383 Usefulness and limitations of sequential serum tryptase for the diagnosis of anaphylaxis in 102
384 patients. Int Arch Allergy Immunol. 2013;160: 192–199. doi:10.1159/000339749
385 11. Brown SGA, Stone SF, Fatovich DM, Burrows SA, Holdgate A, Celenza A, et al. Anaphylaxis:
386 Clinical patterns, mediator release, and severity. J Allergy Clin Immunol. 2013;132: 1141-
387 1149.e5. doi:10.1016/j.jaci.2013.06.015
388 12. Pontarollo G, Mann A, Brandão I, Malinarich F, Schöpf M, Reinhardt C. Protease-activated
389 receptor signaling in intestinal permeability regulation. FEBS Journal. Blackwell Publishing
390 Ltd; 2020. pp. 645–658. doi:10.1111/febs.15055

391 13. Rothmeier AS, Ruf W. Protease-activated receptor 2 signaling in inflammation. Semin
392 Immunopathol. 2012;34: 133–149. doi:10.1007/s00281-011-0289-1
393 14. Zhang R, Ge J. Proteinase-Activated Receptor-2 Modulates Ve-Cadherin Expression to Affect
394 Human Vascular Endothelial Barrier Function. J Cell Biochem. 2017;118: 4587–4593.
395 doi:10.1002/jcb.26123
396 15. Hirano K, Kanaide H. Role of Protease-activated Receptors in the Vascular System. Journal
397 of Atherosclerosis and Thrombosis Review. 2003.
398 16. Trivedi NN, Raymond WW, Caughey GH. Chimerism, point mutation, and truncation
399 dramatically transformed mast cell δ-tryptases during primate evolution. J Allergy Clin
400 Immunol. 2008;121: 1262–1268. doi:10.1016/j.jaci.2008.01.019
401 17. Hunt JE, Stevens RL, Austen KF, Zhang J, Xia Z, Ghildyal N. Natural disruption of the mouse
402 mast cell protease 7 gene in the C57BL/6 mouse. J Biol Chem. 1996;271: 2851–2855.
403 doi:10.1074/JBC.271.5.2851
404 18. Shin K, Watts GFM, Oettgen HC, Friend DS, Pemberton AD, Gurish MF, et al. Mouse mast
405 cell tryptase mMCP-6 is a critical link between adaptive and innate immunity in the chronic
406 phase of Trichinella spiralis infection. J Immunol. 2008;180: 4885–4891.
407 doi:10.4049/jimmunol.180.7.4885
408 19. Fujii W, Kawasaki K, Sugiura K, Naito K. Efficient generation of large-scale genome-

409 modified mice using gRNA and CAS9 endonuclease. Nucleic Acids Res. 2013;41: e187.
410 doi:10.1093/NAR/GKT772
411 20. Subramanian H, Gupta K, Ali H. Roles of MAS-related G protein coupled receptor-X2
412 (MRGPRX2) on mast cell-mediated host defense, pseudoallergic drug reactions and chronic
413 inflammatory diseases. J Allergy Clin Immunol. 2016;138: 700.
414 doi:10.1016/J.JACI.2016.04.051
415 21. Gaudenzio N, Sibilano R, Marichal T, Starkl P, Reber LL, Cenac N, et al. Different activation
416 signals induce distinct mast cell degranulation strategies. J Clin Invest. 2016;126: 3981–3998.
417 doi:10.1172/JCI85538
418 22. Meixiong J, Anderson M, Limjunyawong N, Sabbagh MF, Hu E, Mack MR, et al. Activation
419 of Mast-Cell-Expressed Mas-Related G-Protein-Coupled Receptors Drives Non-histaminergic
420 Itch. Immunity. 2019;50: 1163-1171.e5. doi:10.1016/j.immuni.2019.03.013
421 23. Nakamura T, Fujiwara Y, Yamada R, Fujii W, Hamabata T, Lee MY, et al. Mast cell-derived
422 prostaglandin D2 attenuates anaphylactic reactions in mice. J Allergy Clin Immunol.
423 2017;140: 630-632.e9. doi:10.1016/j.jaci.2017.02.030
424 24. Cui H, Okamoto Y, Yoshioka K, Du W, Takuwa N, Zhang W, et al. Sphingosine-1-phosphate
425 receptor 2 protects against anaphylactic shock through suppression of endothelial nitric oxide
426 synthase in mice. J Allergy Clin Immunol. 2013;132: 1205-1214.e9.

427 doi:10.1016/J.JACI.2013.07.026

428 25. de Matos NA, Lima OCO, da Silva JF, Piñeros AR, Tavares JC, Lemos VS, et al. Blockade of
429 protease-activated receptor 2 attenuates allergenmediated acute lung inflammation and
430 leukocyte recruitment in mice. J Biosci. 2022;47. doi:10.1007/s12038-021-00239-2

431 26. Kawagoe J, Takizawa T, Matsumoto J, Tamiya M, Meek SE, Smith AJH, et al. Effect of
432 Protease-Activated Receptor-2 Deficiency on Allergic Dermatitis in the Mouse Ear. Jpn J
433 Pharmacol. 2002.

434 27. Hox V, Desai A, Bandara G, Gilfillan AM, Metcalfe DD, Olivera A. Estrogen increases the
435 severity of anaphylaxis in female mice through enhanced endothelial nitric oxide synthase
436 expression and nitric oxide production. J Allergy Clin Immunol. 2015;135: 729-736.e5.
437 doi:10.1016/j.jaci.2014.11.003

438 28. Sukocheva OA, Wang L, Albanese N, Pitson SM, Vadas MA, Xia P. Sphingosine kinase
439 transmits estrogen signaling in human breast cancer cells. Mol Endocrinol. 2003;17: 2002–
440 2012. doi:10.1210/me.2003-0119

441 29. Watts VL, Motley ED. Role of Protease-Activated Receptor-1 in Endothelial Nitric Oxide
442 Synthase-Thr495 Phosphorylation. Exp Biol Med. 2009;234: 132–139. doi:10.3181/0807-
443 RM-233

444 30. Tillery LC, Epperson TA, Eguchi S, Motley ED. Featured Article: Differential regulation of

445 endothelial nitric oxide synthase phosphorylation by protease-activated receptors in adult
446 human endothelial cells. Exp Biol Med. 2016;241: 569–580. doi:10.1177/1535370215622584
447 31. Maruyama K, Kagota S, McGuire JJ, Wakuda H, Yoshikawa N, Nakamura K, et al. Enhanced
448 nitric oxide synthase activation via protease-activated receptor 2 is involved in the preserved
449 vasodilation in aortas from metabolic syndrome rats. J Vasc Res. 2016;52: 232–243.
450 doi:10.1159/000442415
451 32. Pham PT, Fukuda D, Yagi S, Kusunose K, Yamada H, Soeki T, et al. Rivaroxaban, a specific
452 FXa inhibitor, improved endothelium-dependent relaxation of aortic segments in diabetic mice.
453 Sci Rep. 2019;9: 1–11. doi:10.1038/s41598-019-47474-0
454 33. Kang N-I, Yoon H-Y, Kim H-A, Kim K-J, Han M-K, Lee Y-R, et al. Protein kinase
455 CK2/PTEN pathway plays a key role in platelet-activating factor-mediated murine
456 anaphylactic shock. J Immunol. 2011;186: 6625–6632. doi:10.4049/JIMMUNOL.1100007
457 34. Mohammad MA, Greenman J, Maraveyas A, Ettelaie C. Activation of PAR2 by tissue factor
458 induces the release of the PTEN from MAGI proteins and regulates PTEN and Akt activities.
459 Sci Rep. 2020;10. doi:10.1038/S41598-020-77963-6
460 35. Imamura T, Dubin A, Moore W, Tanaka R, Travis J. Induction of vascular permeability
461 enhancement by human tryptase: dependence on activation of prekallikrein and direct release
462 of bradykinin from kininogens. Lab Invest. 1996;74: 861–870. Available:

463 https://pubmed.ncbi.nlm.nih.gov/8642782/

464 36. Guilarte M, Sala-Cunill A, Luengo O, Labrador-Horrillo M, Cardona V. The Mast Cell,
465 Contact, and Coagulation System Connection in Anaphylaxis. Front Immunol. 2017;8.
466 doi:10.3389/FIMMU.2017.00846

467 37. Sala-Cunill A, Björkqvist J, Senter R, Guilarte M, Cardona V, Labrador M, et al. Plasma
468 contact system activation drives anaphylaxis in severe mast cell–mediated allergic reactions.
469 Journal of Allergy and Clinical Immunology. 2015;135: 1031-1043.e6.
470 doi:10.1016/J.JACI.2014.07.057

471

472

Supporting information

S1 Fig. Mast cell number and degree of mast cell degranulation in WT and PAR-2 KO mice. (A) Mast cells stained with FITC-avidin in the ears of mice (left) and the number of mast cells (right, n = 3). Magnification, ×200. Bar, 100 μm. (B) Serum histamine concentrations after C48/80 injection (n = 4). (C) Serum mMCP-6 concentrations after C48/80 injection (n = 4). NS, not significant. Data are presented as the mean ± SEM.

S2 Fig. The effect of PAR-2 on vascular hyperpermeability induced by mast cell degranulation. (A) Hematocrit after injection of C48/80 or vehicle in WT or PAR-2 KO mice (n = 4). (B) Evans blue dye leakage in the lungs after systemic injection of C48/80 or vehicle in WT or PAR-2 KO mice (n = 5). (C) Evans blue dye leakage in the ears after local injection of C48/80 or vehicle in WT or PAR-2 KO mice (n = 5). NS, not significant. ***$P < 0.001$. Data are presented as the mean ± SEM.

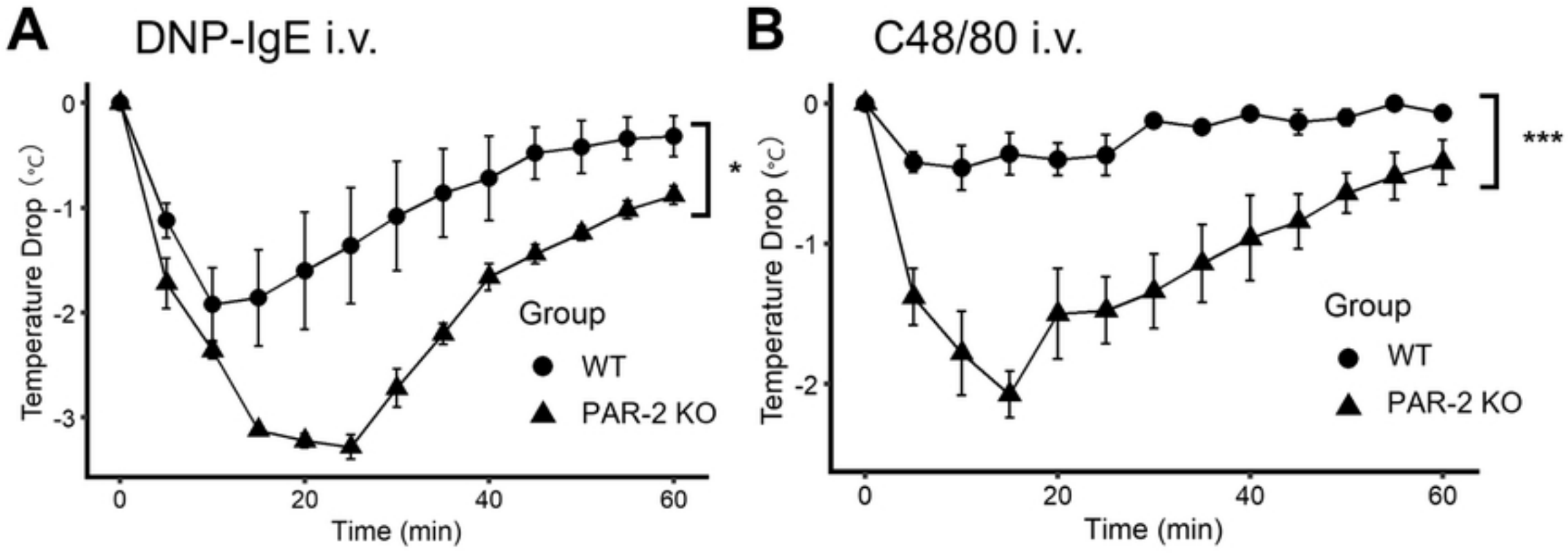
A
DNP-IgE i.v.
Temperature Drop (°C)
0
-1
-2
-3
0
20
40
60
Time (min)
*
Group
WT
PAR-2 KO
B
C48/80 i.v.
Temperature Drop (°C)
0
-1
-2
0
20
40
60
Time (min)
***
Group
WT
PAR-2 KO

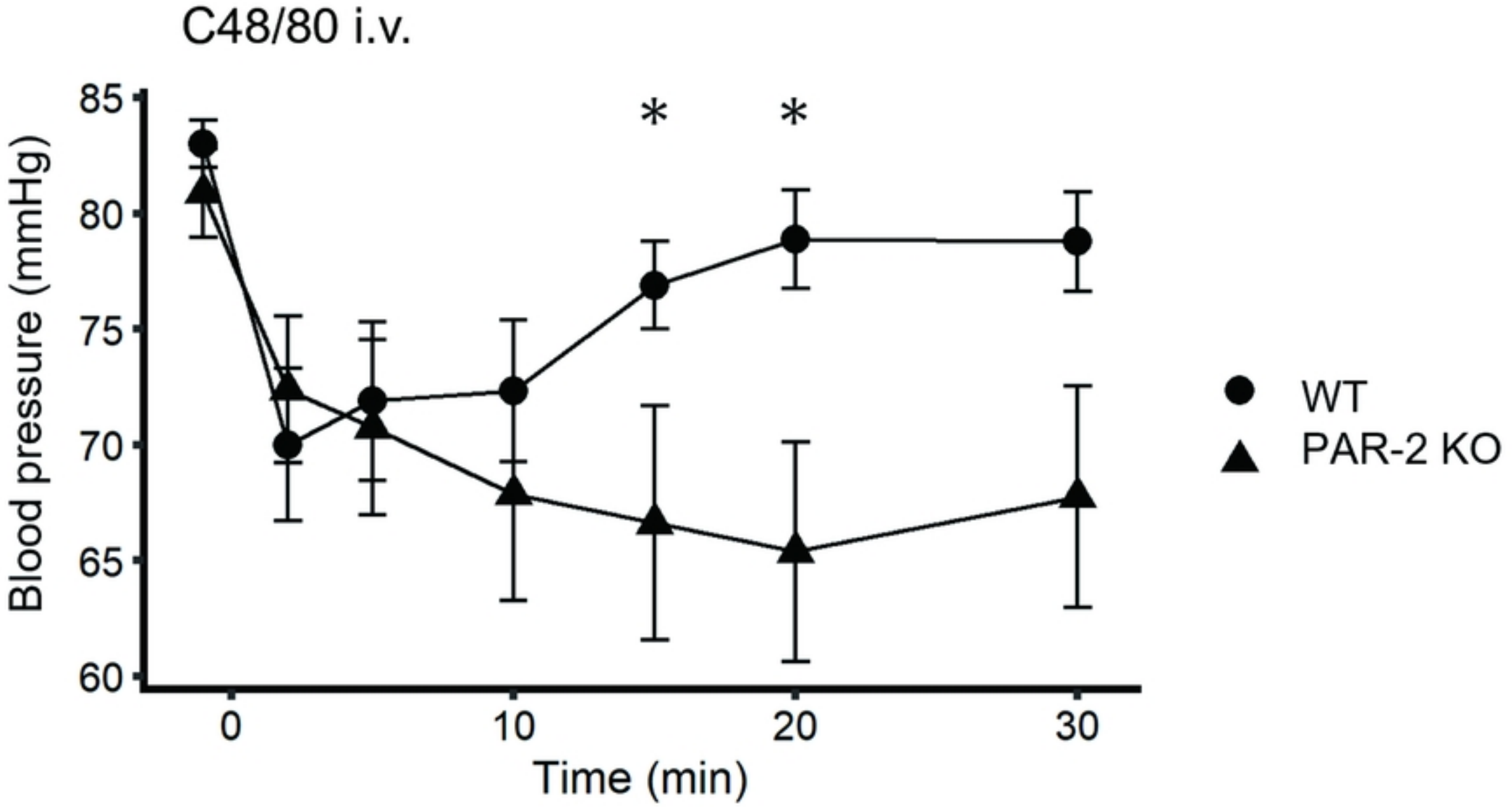
C48/80 i.v.
Blood pressure (mmHg)
85
80
75
70
65
60
*
*
0
10
20
30
Time (min)
WT
PAR-2 KO

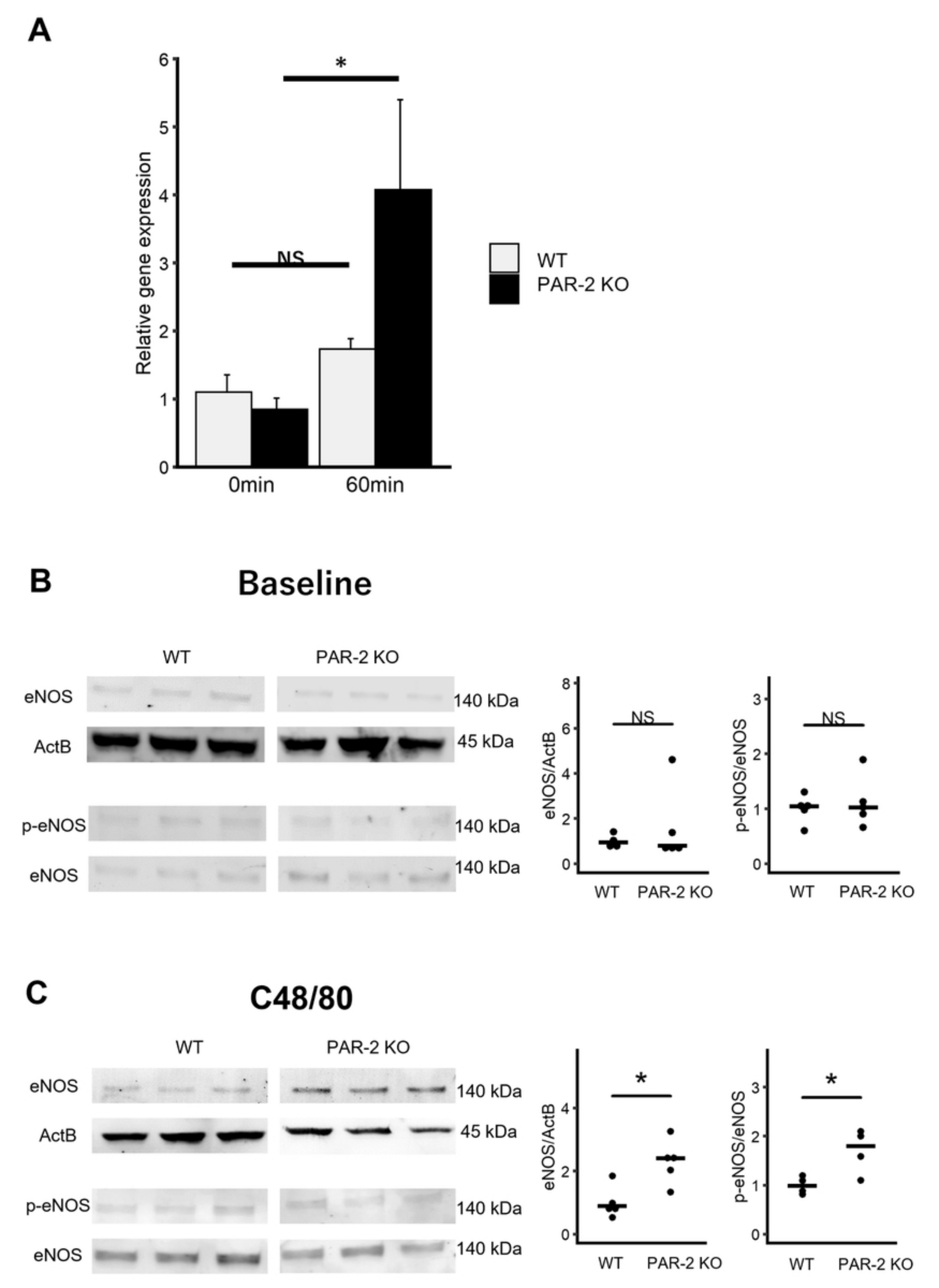
A
Relative gene expression
0
1
2
3
4
5
6
NS
*
0min
60min
WT
PAR-2 KO
B
Baseline
WT
PAR-2 KO
eNOS
ActB
p-eNOS
eNOS
140 kDa
45 kDa
140 kDa
140 kDa
eNOS/ActB
p-eNOS/eNOS
NS
NS
C
C48/80
WT
PAR-2 KO
eNOS
ActB
p-eNOS
eNOS
140 kDa
45 kDa
140 kDa
140 kDa
eNOS/ActB
p-eNOS/eNOS
*
*

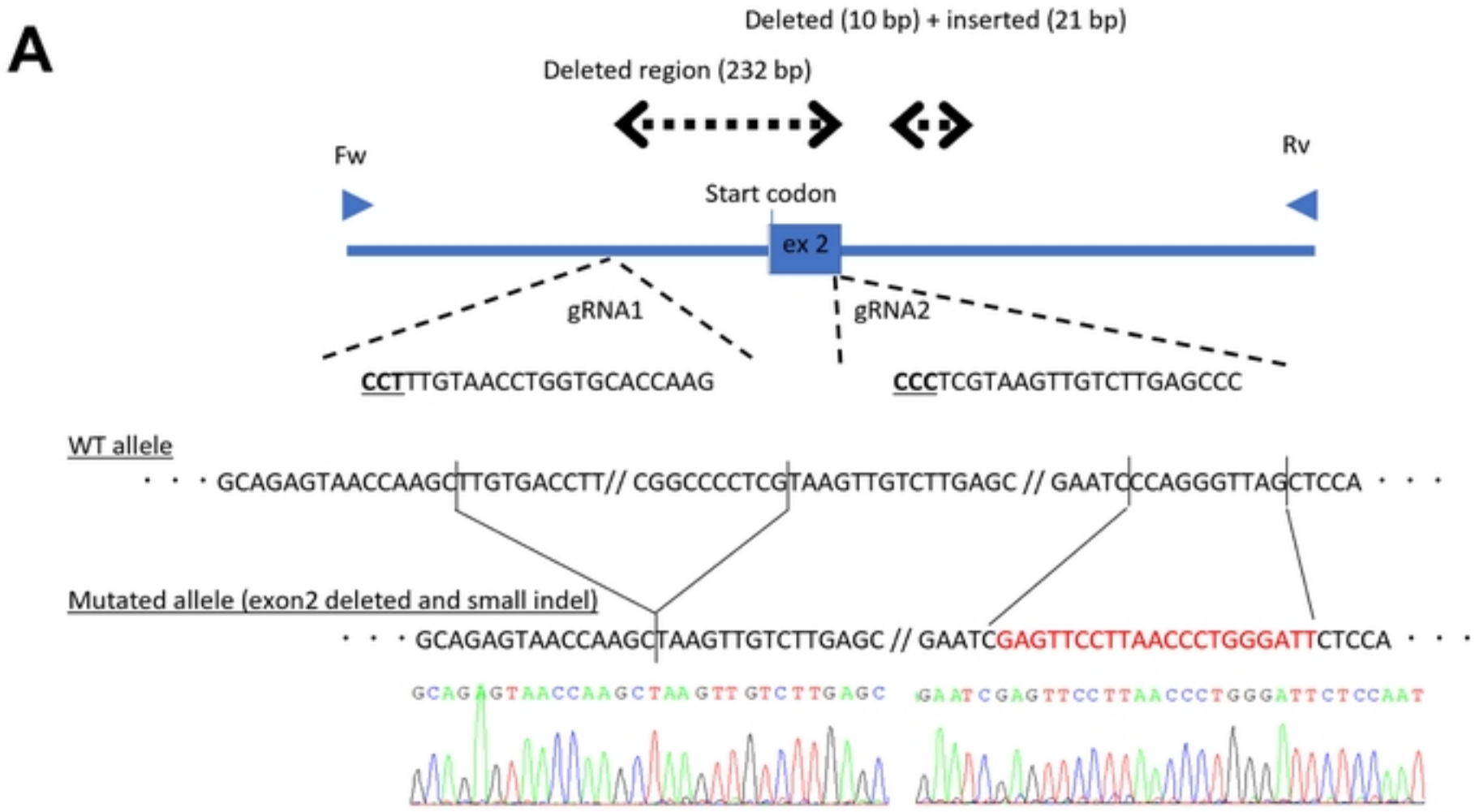
A
Deleted (10 bp) + inserted (21 bp)
Deleted region (232 bp)
Fw
Rv
Start codon
ex 2
gRNA1
gRNA2
CCTTTGTAACCTGGTGCACCAAG
CCCTCGTAAGTTGTCTTGAGCCC
WT allele
· · · GCAGAGTAACCAAGCTTGTGACCTT// CGGCCCCTCGTAAGTTGTCTTGAGC // GAATCCCAGGGTTAGCTCCA · · ·
Mutated allele (exon2 deleted and small indel)
· · · GCAGAGTAACCAAGCTAAGTTGTCTTGAGC // GAATCGAGTTCCTTAACCCTGGGATTCTCCA · · ·

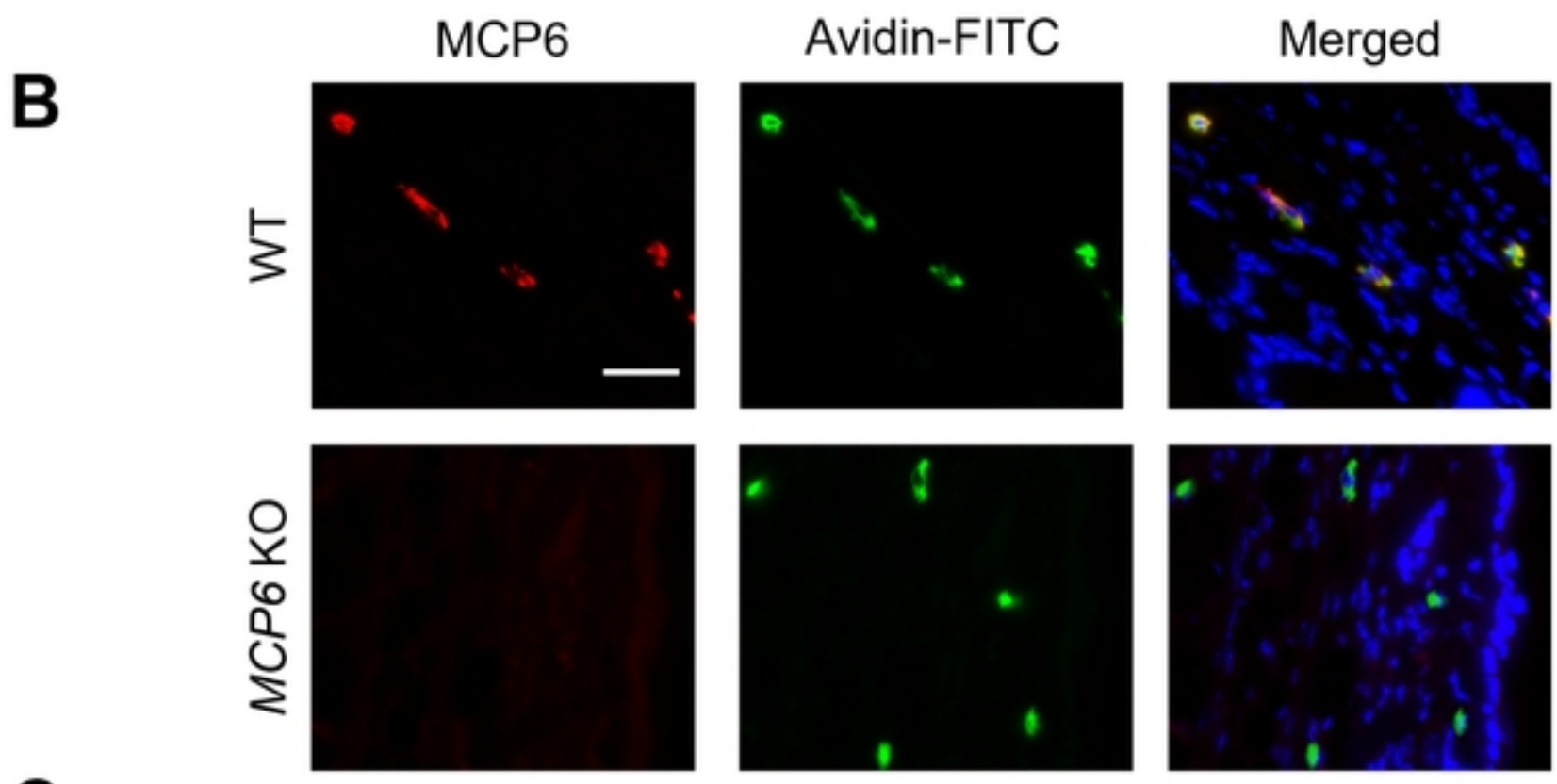
B
MCP6
Avidin-FITC
Merged
WT
MCP6 KO

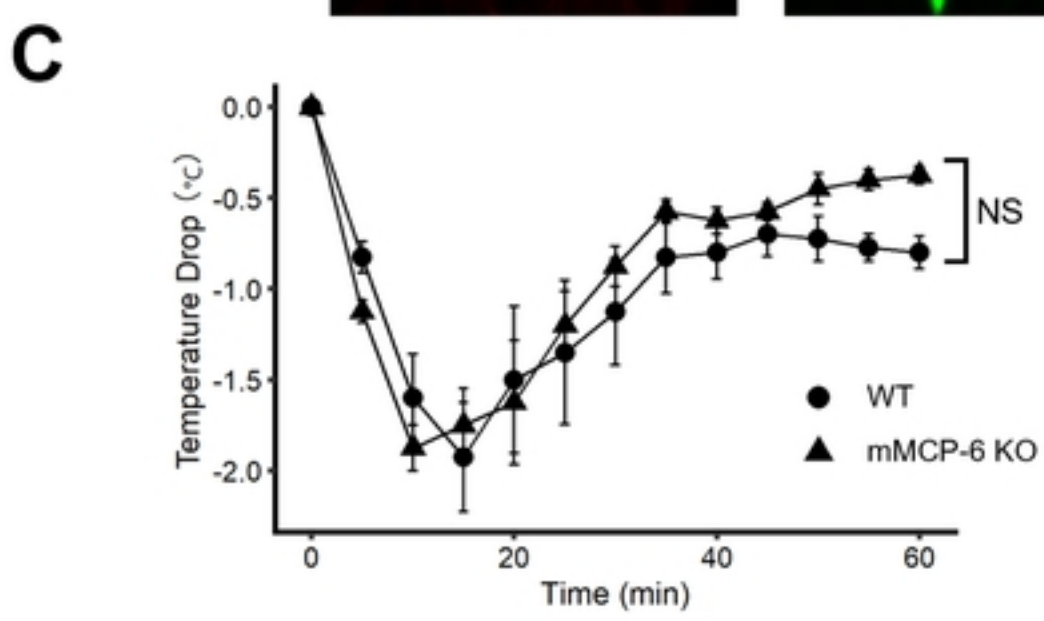
C
Temperature Drop (°C)
Time (min)
NS
WT
mMCP-6 KO

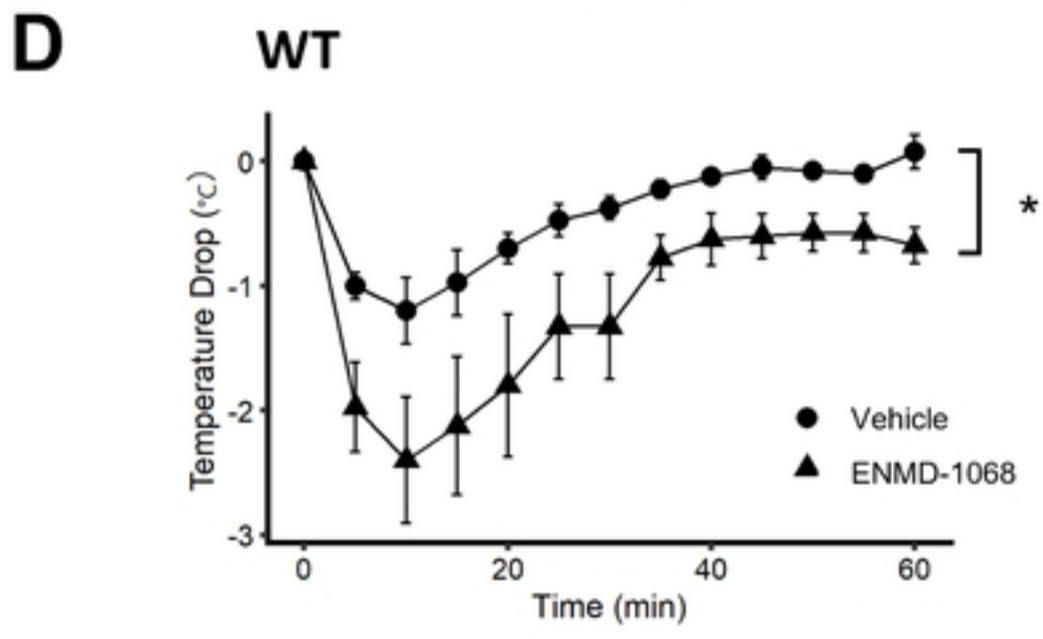
D
WT
Temperature Drop (°C)
Time (min)
*
Vehicle
ENMD-1068

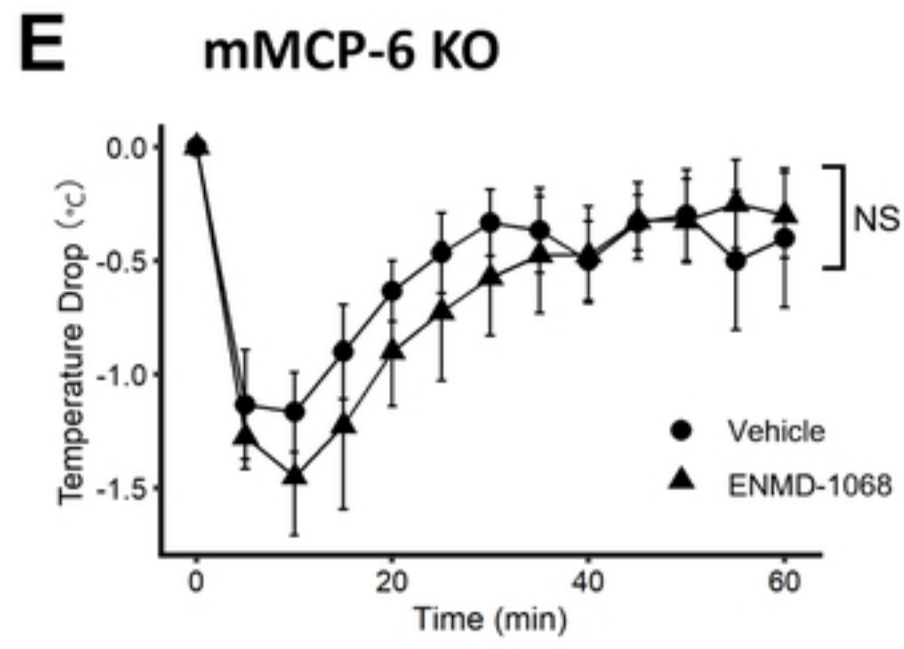
E
mMCP-6 KO
Temperature Drop (°C)
Time (min)
NS
Vehicle
ENMD-1068